NASA TECHNICAL REPORT

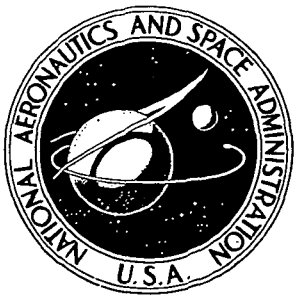

NASA TR R-395

NASA TR R-395

A STUDY OF BERYLLIUM AND BERYLLIUM-LITHIUM COMPLEXES IN SINGLE-CRYSTAL SILICON

by Roger K. Crouch, James B. Robertson, and T. E. Gilmer, Jr.

Langley Research Center
Hampton, Va. 23365

NATIONAL AERONAUTICS AND SPACE ADMINISTRATION • WASHINGTON, D. C. • DECEMBER 1972

1. Report No. NASA TR R-395	2. Government Accession No.	3. Recipient's Catalog No.
4. Title and Subtitle A STUDY OF BERYLLIUM AND BERYLLIUM-LITHIUM COMPLEXES IN SINGLE-CRYSTAL SILICON		5. Report Date December 1972 6. Performing Organization Code
7. Author(s) Roger K. Crouch, James B. Robertson, and T. E. Gilmer, Jr.		8. Performing Organization Report No. L-8545
9. Performing Organization Name and Address NASA Langley Research Center Hampton, Va. 23365		10. Work Unit No. 502-03-51-02 11. Contract or Grant No.
12. Sponsoring Agency Name and Address National Aeronautics and Space Administration Washington, D.C. 20546		13. Type of Report and Period Covered Technical Report 14. Sponsoring Agency Code

15. Supplementary Notes

The information presented herein is based on a thesis submitted by Roger K. Crouch in partial fulfillment of the requirements for the degree of Doctor of Philosophy in Physics, Virginia Polytechnic Institute and State University, Blacksburg, Virginia, 1971.

T. E. Gilmer, Jr., is Professor of Physics, VPI and S.U.

16. Abstract

When beryllium is thermally diffused into silicon, it gives rise to acceptor levels 191 meV and 145 meV above the valence band. Quenching and annealing studies indicate that the 145-meV level is due to a more complex beryllium configuration than the 191-meV level. When lithium is thermally diffused into a beryllium-doped silicon sample, it produces two new acceptor levels at 106 meV and 81 meV. Quenching and annealing studies indicate that these new levels are due to lithium forming a complex with the defects responsible for the 191-meV and 145-meV beryllium levels, respectively. Electrical measurements imply that the lithium impurity ions are physically close to the beryllium impurity atoms. The ground state of the 106-meV beryllium-lithium level is split into two levels, presumably by internal strains. Tentative models are proposed to explain these results.

17. Key Words (Suggested by Author(s))	18. Distribution Statement
Impurity complexes in silicon Beryllium impurities Lithium impurities Infrared absorption	Unclassified – Unlimited

19. Security Classif. (of this report)	20. Security Classif. (of this page)	21. No. of Pages	22. Price*
Unclassified	Unclassified	31	$3.00

*For sale by the National Technical Information Service, Springfield, Virginia 22151

A STUDY OF BERYLLIUM AND BERYLLIUM-LITHIUM COMPLEXES IN SINGLE-CRYSTAL SILICON*

By Roger K. Crouch, James B. Robertson,
and T. E. Gilmer, Jr.**
Langley Research Center

SUMMARY

When beryllium is thermally diffused into silicon, it gives rise to acceptor levels 191 meV and 145 meV above the valence band. Quenching and annealing studies indicate that the 145-meV level is due to a more complex beryllium configuration than the 191-meV level. When lithium is thermally diffused into a beryllium-doped silicon sample, it produces two new acceptor levels at 106 meV and 81 meV. Quenching and annealing studies indicate that these new levels are due to lithium forming a complex with the defects responsible for the 191-meV and 145-meV beryllium levels, respectively. Electrical measurements imply that the lithium impurity ions are physically close to the beryllium impurity atoms. The ground state of the 106-meV beryllium-lithium level is split into two levels, presumably by internal strains. Tentative models are proposed to explain these results.

INTRODUCTION

Technological advancements in recent years have led to an ever increasing demand for new and better solid-state electronic devices. To assist in the development of such devices, numerous studies on the electrical (refs. 1 to 4) and optical (refs. 5 to 8) properties of the basic semiconducting materials have been carried out. As the technology progressed in growing and purifying single-crystal silicon, it became possible to introduce various concentrations of specific impurities into the crystal and then to catalog the properties of the silicon containing the known impurity. Initially, it was found that Group V impurities produced n-type silicon and Group III impurities produced p-type silicon. It was shown that effective-mass theory (refs. 9 to 12) gave excellent agreement between predicted and measured values for the excited-state spectra of shallow donors,

*The information presented herein is based on a thesis submitted by Roger K. Crouch in partial fulfillment of the requirements for the degree of Doctor of Philosophy in Physics, Virginia Polytechnic Institute and State University, Blacksburg, Virginia, 1971.

**Professor of Physics, VPI and S.U., Blacksburg, Va.

that is, Group V impurities. (Shallow impurity states, either donor or acceptor, are those bound states whose binding energy is much less than band-gap energy.) The rather large discrepancies between predicted and observed ground-state energies were understandable due to the simplified potential assumed in effective-mass theory (refs. 12 and 13). When effective-mass theory was applied to shallow acceptors, it gave relatively good qualitative predictions for the excited states but it did not give good quantitative values. Acceptor states are quite complicated, and the theory is still undergoing development (refs. 14 and 15).

Other studies showed that oxygen was present in large quantities in Czochralski-grown silicon; but the oxygen was electrically inactive in most cases and only modified the infrared-absorption spectra of silicon by introducing vibrational absorptions, primarily around 9 μm (refs. 16 and 17). The oxygen almost certainly occupied an interstitial lattice site in one of the six equivalent sites around a silicon-silicon bond (ref. 18).

When lithium is introduced as an impurity in silicon, it forms a complex with the oxygen which alters the electrical and optical properties (refs. 19 to 21). The lithium occupies a tetrahedral, interstitial position and is described by effective-mass theory (ref. 21). In float-zone silicon, oxygen content less than 10^{16} cm^{-3}, the lithium gives rise to an energy level 32 meV below the conduction band. In Czochralski silicon, oxygen content typically 10^{18} cm^{-3}, the lithium energy level is located 39 meV below the conduction band. Further studies indicate that the 9-μm vibrational absorption of the interstitial oxygen is shifted to about 10 μm (ref. 22). Lithium has also been used to compensate heavily doped p-type silicon in order to reduce free-carrier absorption and to study pair formation between lithium and boron. Vibrational absorptions have been found which have an isotopic dependency on the lithium and the boron, and a tentative model has been presented for the lithium-boron complex (refs. 23 to 25). Some recent work deals with vibrational absorptions due to carbon and carbon-oxygen impurities in silicon (ref. 26).

Group II impurities such as zinc and beryllium have been studied in germanium (refs. 27 to 29) and have been found to produce acceptor levels which, to a first approximation, can be described by a helium model. (A helium model is essentially a system which can be treated as a doubly charged nucleus with two carriers (either holes or electrons depending on the nuclear charge) bound to it at low temperatures. The first electron (hole) will have excited-state energies comparable to those predicted by the hydrogen model; the second electron (hole) will have a ground-state energy about four times deeper than the first electron. Also, the energy spacings between the excited states of the second electron will be larger by a factor of four.) The Group II impurities, magnesium and beryllium, have been studied in silicon (refs. 30 to 34). It is interesting to note that the magnesium produces n-type silicon and occupies an interstitial lattice site, while beryllium produces p-type silicon and is therefore believed to occupy a

substitutional lattice site. Magnesium introduces two related donor states described by a helium model. Beryllium introduces two independent series of infrared absorptions, which are separated by about 40 meV, neither of which seem to have the associated, deeper level expected for the helium model. (While it is uncommon for an impurity to produce two independent levels, beryllium is not unique in this respect since sulfur introduces at least two independent donor levels. See ref. 35.) When lithium is introduced into a beryllium-doped silicon sample, two new series of infrared absorptions are found at energies closer to the valence-band edge, indicating lithium forms a complex with the beryllium.

A study of the electrical and optical properties of beryllium and beryllium-lithium complexes in silicon was done to better understand the unusual properties associated with these impurities. The results of this study are presented and discussed in the present paper. Tentative models for the two beryllium and the two beryllium-lithium impurity sites are proposed.

SYMBOLS

$D_{jj'}^{\alpha\beta}$ numerical constants (eq. (6))

∇^2 Laplacian operator, $\frac{\partial^2}{\partial x^2} + \frac{\partial^2}{\partial y^2} + \frac{\partial^2}{\partial z^2}$ in rectangular Cartesian coordinates

e electronic charge

E energy level of shallow donor

E_A acceptor ionization energy

$F_j(\vec{r})$ hydrogenlike envelope wave function

$\hbar = \frac{\text{Planck constant}}{2\pi}$

I light intensity

I_0 incident light intensity

J total angular momentum quantum number

$\vec{k}$ wave vector

m	effective mass of charge carrier
m_0	rest mass of electron
m_l	longitudinal effective mass
m_t	transverse effective mass
n	free-carrier concentration
$\vec{r}$	radial vector
R	reflectivity of sample surface
R_H	Hall coefficient
t	sample thickness
T	temperature
$U(\vec{r})$	Coulomb potential due to interaction between electron and impurity ion
$V(\vec{r})$	periodic potential of an electron in a perfect silicon lattice
α	absorption coefficient (eq. (7))
α_j	weighting factor for relative contribution of each equivalent minimum
ϵ_j	parameter (eq. (6))
κ	dielectric constant
λ	spin-orbit splitting of valence bands at $\vec{k} = 0$
μ_H	Hall mobility
ρ	resistivity
τ	percent transmission

$\varphi_j(\vec{r})$ Bloch wave function at the jth conduction band minimum

$\psi(\vec{r})$ donor-state wave function

$\psi_i(\vec{r})$ impurity wave function

SHALLOW IMPURITY STATES IN SILICON

Donors

When Group V elements are placed into a substitutional silicon lattice site, four of the electrons in the outer shell of the impurity atom are needed to complete the covalent bonds with the four adjacent silicon atoms. The fifth electron, however, is bound by a Coulomb attraction to the remaining charge on the impurity ion. If this system is treated as a hydrogen atom, where the potential energy of the electron is modified by the dielectric constant of the material and effective mass replaces the free-electron mass, then the excited-state spectrum associated with the impurity should be observed in the far infrared. Experimental data on the Group V impurities, phosphorus, antimony, and arsenic, convincingly demonstrate the existence of bound states as demanded by the hydrogen model for donors.

The Schrödinger equation for the donor-state wave functions has the form

$$\left[-\frac{\hbar^2}{2m}\nabla^2 + V(\vec{r}) + U(\vec{r})\right]\psi(\vec{r}) = E\psi(\vec{r}) \tag{1}$$

where $V(\vec{r})$ is the periodic potential of an electron in a perfect silicon lattice and $U(\vec{r})$ is the additional potential due to the impurity ion. For large r

$$U(\vec{r}) = -\frac{e^2}{\kappa r} \tag{2}$$

where $\kappa \approx 12$ is the dielectric constant of silicon. In silicon, the energy-band structure of the conduction band has been found to have six equivalent minimums located along the <100> directions in $\vec{k}$ space (ref. 12). It has been shown by Kohn and Luttinger (ref. 9) that the impurity wave functions have the approximate form

$$\psi_i(\vec{r}) = \sum_{j=1}^{6} \alpha_j F_j(\vec{r})\varphi_j(\vec{r}) \qquad (i = 1, \ldots, 6) \tag{3}$$

where $\varphi_j(\vec{r})$ is the Bloch wave function at the jth conduction band minimum and α_j are the numerical coefficients which describe the relative contributions of each of the six equivalent minimums. The $F_j(\vec{r})$ is a hydrogenlike envelope wave function which, for a

band minimum in the <001> direction, satisfies the following effective-mass wave equation:

$$\left[-\frac{\hbar^2}{2m_t}\left(\frac{\partial^2}{\partial x_j^2}+\frac{\partial^2}{\partial y_j^2}\right)-\frac{\hbar^2}{2m_l}\frac{\partial^2}{\partial z_j^2}-\frac{e^2}{\kappa r}\right]F_j(\vec{r})=EF_j(\vec{r}) \tag{4}$$

where $m_t = 0.19m_0$ and $m_l = 0.98m_0$ (ref. 36).

When various Group V impurities are observed experimentally, the excited-state structure observed in the spectra are in excellent agreement with theoretical predictions resulting from approximate solutions of equations (4). Since the orbits of these excited states are quite large, the potential in equation (2) should describe the situation very well. However, the value of the ground-state energy is different for different impurities; but this is not unexpected, since for small values of r the assumption of a screened ion potential is very poor. Local strains, a varying dielectric constant, and numerous other complications arise in the immediate vicinity of the impurity ion. There are no adequate theories to predict the ground-state energies of the various impurities.

Acceptors

When Group III impurities are placed on substitutional lattice sites in silicon, the unsatisfied covalent bond associated with one of the adjacent silicon atoms is an available electron state which can accept an electron from the valence band. When an electron is taken from the valence band, the resulting positively charged hole will have a Coulomb attraction for the negatively charged impurity ion. Thus, an effective-mass hydrogen model can also be used to describe the acceptor states. While these states are analogous to the donor states in a general way, the theory must incorporate the complexity of the valence band near its maximum at $\vec{k} = 0$ (see fig. 1).

If spin is not included, the band is threefold degenerate at $\vec{k} = 0$; but when spin is included, the resulting sixfold degeneracy is split by the spin-orbit interaction into a fourfold degenerate $p_{3/2}$ band and a twofold degenerate $p_{1/2}$ band. The $p_{3/2}$ band corresponds to the atomic $J = 3/2$ states, and the $p_{1/2}$ band corresponds to atomic $J = 1/2$ states.

Because of the nature of this degeneracy (i.e., the fact that three different bands are involved), the effective-mass theory is more complicated for acceptors than for donors in silicon. Kohn (ref. 12) has treated the problem for silicon and found that the total wave functions of the acceptor states have structures given approximately by

$$\psi_k(\vec{r}) = \sum_{j=1}^{6} F_j^k(\vec{r})\varphi_j(\vec{r}) \tag{5}$$

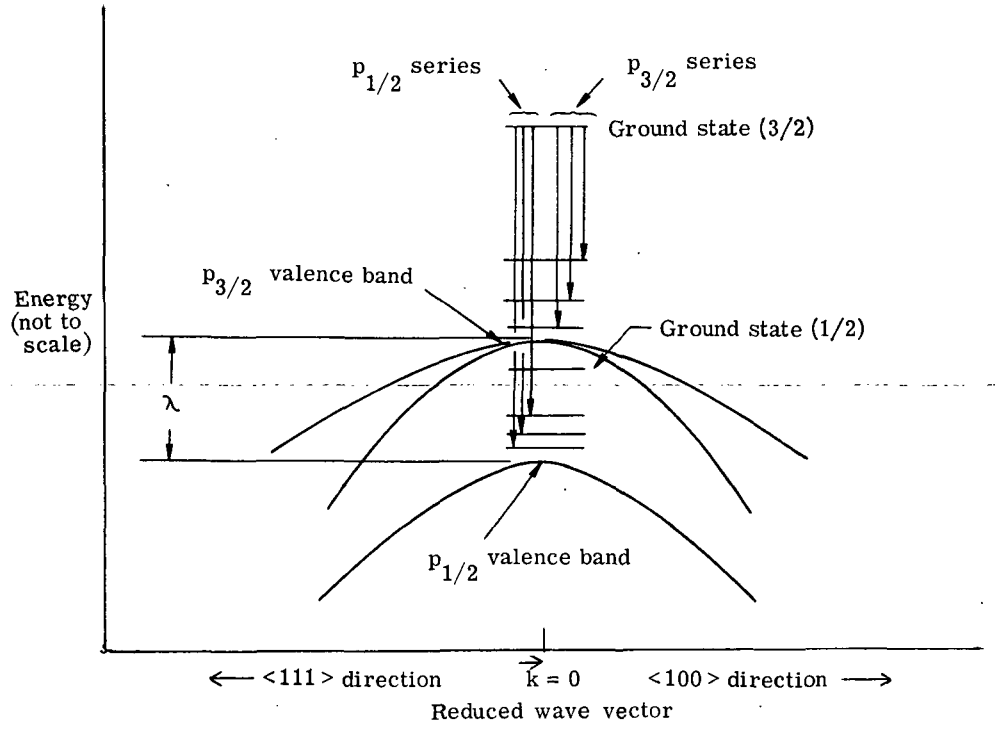

Figure 1.- The spin-orbit split valence band of silicon with associated acceptor states; λ is the spin-orbit splitting at $\vec{k} = 0$; $\lambda \approx 44$ meV.

where $F_j^k(\vec{r})$ are hydrogenlike envelope functions modifying the Bloch functions $\varphi_j(\vec{r})$. The index k distinguishes the degenerate functions among the impurity states, and the functions $F_j(\vec{r})$ are determined by the following six coupled hydrogenlike effective-mass wave functions:

$$\sum_{j'=1}^{6} D_{jj'}^{\alpha\beta}\left(\frac{1}{i}\frac{\partial}{\partial x^\alpha}\right)\left(\frac{1}{i}\frac{\partial}{\partial x^\beta}\right)F_{j'}(\vec{r}) + \frac{e^2}{\kappa r}F_j(\vec{r}) = \left(E + \lambda\epsilon_j\right)F_j(\vec{r}) \qquad \begin{pmatrix} j = 1, 2, \ldots, 6 \\ \alpha,\beta = 1, 2, 3 \end{pmatrix} \tag{6}$$

where $D_{jj'}^{\alpha\beta}$ are numerical constants characteristic of the material and have dimensions of $\hbar^2/m$; $\epsilon_j = 0$ for $j = 1$ to 4 and $\epsilon_j = 1$ for $j = 5$ to 6. It may be shown that if λ were very large compared to E, the six equations would separate into four equations associated solely with the $p_{3/2}$ states and two equations associated solely with the $p_{1/2}$ states. In germanium, the spin-orbit splitting is about 30 times larger than the ionization energy, and only four equations are required to describe the acceptor states. For silicon, the energy of the acceptor states is on the order of 40 to 200 meV and λ is on the order of 40 meV; therefore, the wave functions of all six valence bands will enter with appreciable amplitude into the total wave function of the acceptor states in silicon.

When the experimental infrared-absorption data are compared to the theoretical predictions, the agreement is qualitatively good; but there are small differences in the spacings of the excited-state spectra for different impurities (fig. 2(a)). Also, as in the case of donors, the assumption of constant κ is invalid for small values of r; therefore, the depth of the ground state is chemically dependent. The acceptor-state equations for silicon, as is also the case for germanium, have been solved only approximately by variational techniques. However, it turns out that the theory and experiment do not agree as well for acceptor states in silicon as for these states in germanium, presumably due to the complexity introduced by the small value of the spin-orbit splitting in silicon.

As previously mentioned, the top of the $p_{3/2}$ valence band is fourfold degenerate. Many of the bound states associated with it are also fourfold degenerate. When external stresses are applied to silicon, the degeneracy of the localized states may be partially lifted. If the stress is applied uniaxially along the major axes of the crystals, it is theoretically possible to determine the degeneracies of the ground states and the excited

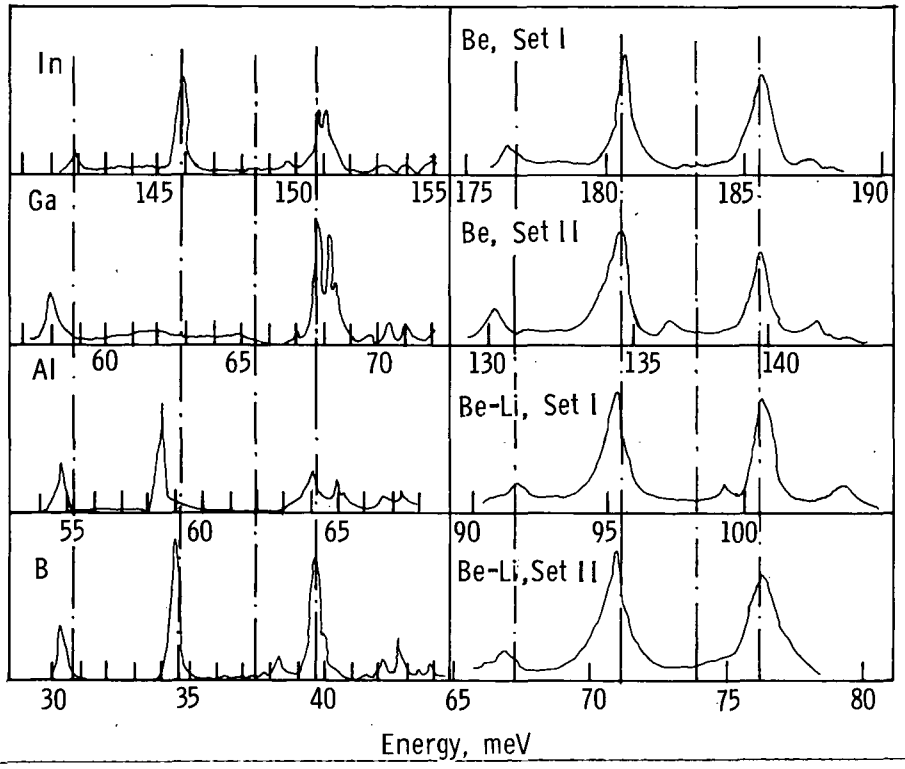

(a) Lines associated with shallow acceptors (ref. 8).

(b) Lines associated with beryllium complexes.

Figure 2.- Absorption spectra of Group III impurities and the beryllium associated impurities. Vertical lines indicate the predicted location of lines using effective-mass theory; all ordinate values are schematic representations of relative absorption intensities.

states. Onton, Fisher, and Ramdas (ref. 8) have studied the Group III impurities (boron, aluminum, gallium, and indium) in silicon by using these techniques. They have shown that all of these impurities are located in a tetrahedral lattice position. The ground state associated with this position is fourfold degenerate; and when stresses of sufficient magnitude are applied, the level is split into two twofold degenerate levels.

This section has presented a brief review of the theory for shallow impurity states in silicon. The ionization energies associated with the impurities reported here are large enough compared to the band gap energy to cause doubt as to the applicability of shallow-acceptor theory; however, the excited-state spectra of all the impurities studied appear to be in excellent agreement with the Group III impurities (see fig. 2). Because of this, at least the beryllium-associated impurity excited states have been regarded as shallow impurity states.

DESCRIPTION OF THE EXPERIMENT

Optical Studies

Both Czochralski and float-zone single-crystal silicon (ref. 36) were used in preparing the test samples. Table 1 lists each sample reported, along with its method of growth, predominant impurity, resistivity prior to and after doping, doping time and temperature. The samples were polished disks 25.4 mm in diameter, and the thickness varied from about 0.5 mm up to 3.0 mm. Infrared-absorption spectra were obtained over a range from 1.0 to 50 μm using two grating spectrophotometers. Both instruments were purged by dry air during all runs (ref. 37).

TABLE 1.- GENERAL INFORMATION ABOUT SAMPLES

Sample identification	Data presented in figure	Method of growth (a)	Major impurity prior to doping (a)	Resistivity prior to beryllium doping, Ω-cm (a)	Beryllium doping		Resistivity after beryllium doping, Ω-cm (a)
					Time, hr	Temperature, °C	
269-4	5, 6	Float-zone	Boron	100	1	1300	0.3
X-9	7, 8(b), 9	Float-zone	Phosphorus	100	1	1300	.25
858-13	8(a)	Float-zone	Phosphorus	800	1	1300	---
Ox-11	10	Czochralski	Boron	140	2	1320	---
X-10	11, 12	Float-zone	Phosphorus	100	1	1300	.2
Ox-4	13	Czochralski	Boron	140	2	1340	.4
422-14	14	Float-zone	Boron	260	$1\frac{1}{4}$	1340	.2
957-23	15	Float-zone	Boron	380	1	1300	.5

[a] Information supplied by manufacturer.

The infrared spectroscopy was performed at temperatures less than 20 K for all figures presented in this report unless otherwise noted in the figure. The low temperature of the samples was attained through the use of a liquid helium Dewar in which the sample was clamped into a copper sample holder that was in contact with the cryogenic liquid. The temperature of the samples was not controlled in most cases and varied from around 8 K to 20 K depending upon the impurity concentration, thickness of the sample, and grade of thermal contact. Sample temperatures were measured with a commercially available germanium resistance thermometer. A piece of germanium was sealed inside a small copper block with a helium transfer gas inside. Four wires were mounted on the germanium to measure the resistance which had been previously calibrated as a function of temperature. The copper block was mounted against the silicon by using vacuum grease.

All plots of optical data are presented in terms of percent transmission, rather than absorption coefficient, as a function of wave number. Since the absorptions are very strong in most cases, errors in percent transmission (up to 5 units) would lead to large errors in absorption coefficient (ref. 5). It can be shown that the absorption coefficient α is related to the light intensity by

$$I = I_0 \frac{(1 - R)^2 \exp(-\alpha t)}{1 - R^2 \exp(-2\alpha t)} \tag{7}$$

where I is the intensity of the beam after passing through the sample, I_0 is the incident beam intensity, R is the reflectivity of the sample surface, and t is the sample thickness. The transmission τ is the ratio of the intensities

$$\tau = \frac{I}{I_0} = \frac{(1 - R)^2 \exp(-\alpha t)}{1 - R^2 \exp(-2\alpha t)} \tag{8}$$

Solving equation (8) for α gives

$$\alpha = \ln\left[\frac{(1 - R)^2 + \sqrt{(1 - R)^4 + 4\tau^2 R^2}}{2\tau}\right] t^{-1} \tag{9}$$

It is readily seen from equation (9) that if $R \ll 1$, α varies as the logarithm of the reciprocal of the transmission. Therefore, as τ approaches zero, it can become very important that measurements of τ become more accurate; yet, the sensitivity of the experimental setup is such that more accurate values of percent transmission cannot be measured. Since the present study deals primarily with energy locations and relative absorption strengths, values of absorption coefficients would not lead to any significant new conclusions and percent-transmission measurements would be just as informative.

Electrical Measurements

Hall samples were cut in the standard bridge shape shown in figure 3. Contacts to the samples were made by sputtering aluminum on the tabs and annealing at 600° C for 15 minutes to form an eutectic bond between the aluminum and silicon. The leads were

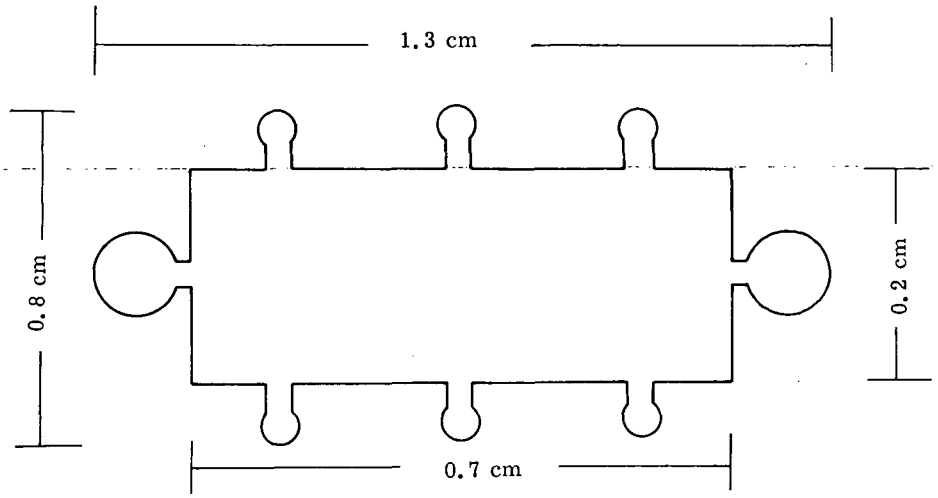

Figure 3.- Typical Hall shape with dimensions.

soldered to the aluminum-coated tabs with indium solder and a tesla coil was arced to each tab to help break down any rectifying contacts that still remained. Resistivity and Hall coefficient were determined in a manner essentially the same as that described in reference 19. Measurements were taken reversing both current and magnetic field to reduce error. The magnetic field used for the Hall measurements was 2740 G.

The resistivity of the optical samples prior to polishing was measured by a four-point probe as explained by Valdes in reference 38. The resistivity of some optical samples was not measured due to difficulty in establishing good electrical contacts.

Doping Procedures

Beryllium.- Beryllium was thermally diffused into the silicon using the so-called sandwich method of reference 30. A layer of beryllium was vapor deposited onto each silicon wafer. Two or more wafers were stacked with the plated sides adjacent and placed in a helium environment at temperatures of 1300° C to 1340° C for 1 to 2 hr (see table 1). The wafers were welded together during the doping procedure and had to be sawed apart.

Lithium.- The most efficient way to introduce the lithium was to plate a so-called dummy wafer on both sides with lithium and sandwich this dummy between two beryllium-

doped wafers. The sandwich was placed in a helium environment and heated at 600° C for 30 min. The two outer wafers were then turned over and heated for another 30 min. The lithium-plated wafer was then removed, and the two doped wafers were annealed at 600° C for 30 min to assure a more uniform doping.

Annealing and Quenching Procedures

Samples to be annealed were placed between two high-purity wafers of silicon in a helium environment. This was done to reduce surface chemical reactions between stray impurities in the system and the doped sample.

For quenching, the samples were held against a cylindrical piece of graphite by means of a reduced pressure inside the graphite cylinder (see fig. 4). A thermocouple was placed against the silicon to allow temperature monitoring. This system was placed in a cylindrical quartz tube with a nitrogen gas stream flowing by the sample. The graphite was heated by means of an rf heater until the wafer reached the desired temperature where it was held for about 3 to 5 min and dropped into a liquid nitrogen bath. In all cases the samples were brought back to room temperature before mounting in the cryostat.

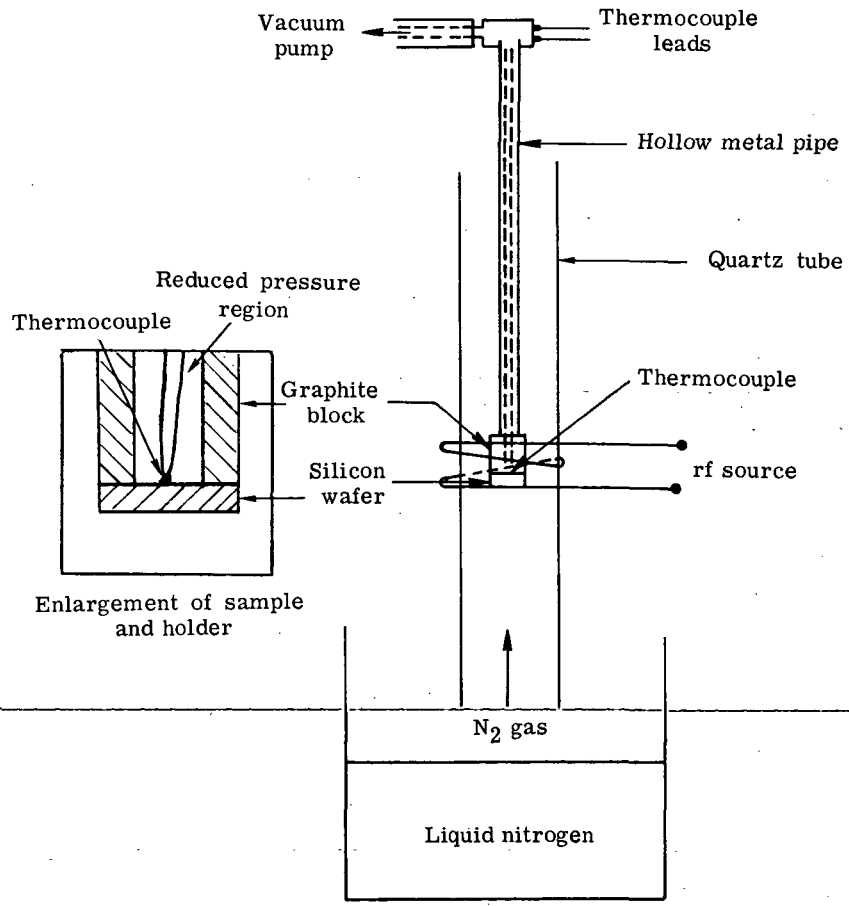

Figure 4.- Quenching arrangement.

RESULTS AND DISCUSSION

Beryllium

When beryllium is thermally diffused into silicon, the resultant p-type material is a consequence of acceptor levels having an ionization energy of about 170 meV as determined from Hall effect measurements. The parameter plotted in figure 5 is derived from Hall

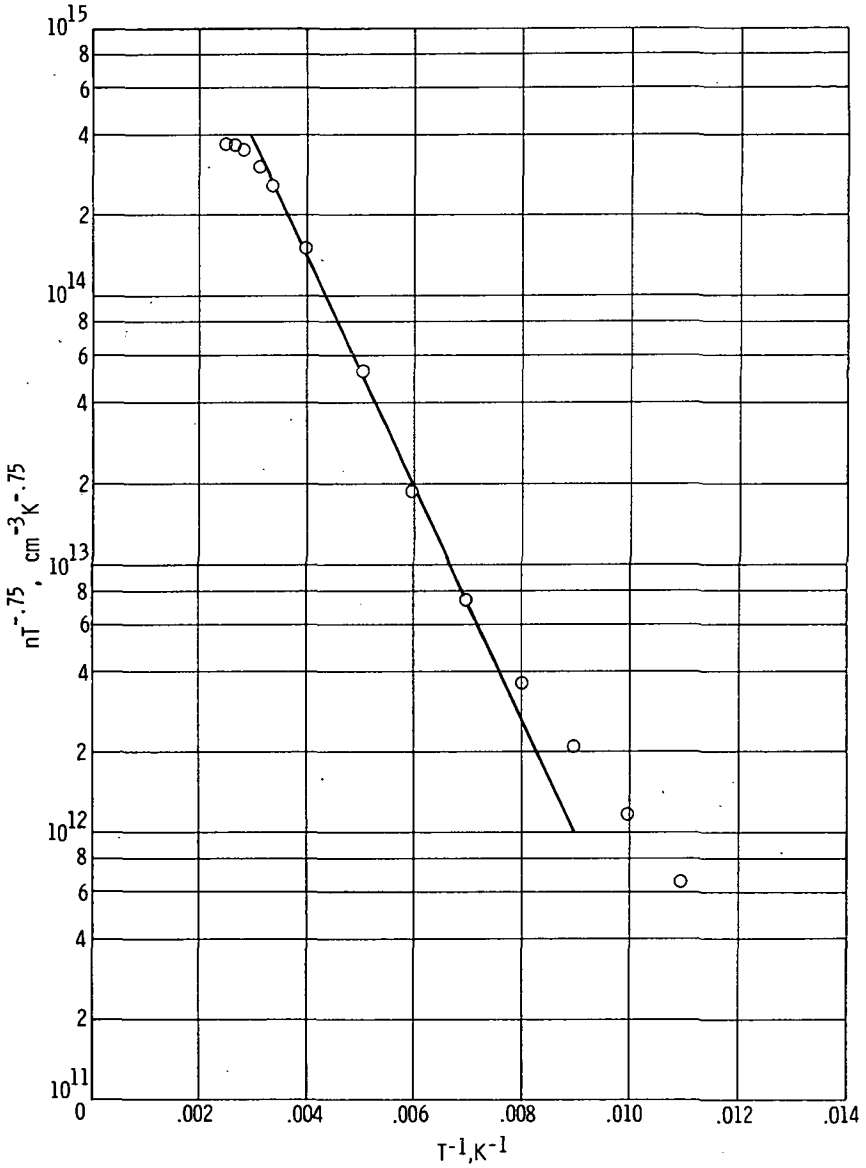

Figure 5.- Parameter containing carrier concentration and temperature as a function of temperature for beryllium-doped silicon.

coefficient calculations, and the slope of the curve in the intermediate temperature region is directly proportional to the ionization energy. Hall mobility,

$$\mu_H = \frac{R_H}{\rho} \tag{10}$$

as a function of temperature typically behaves as shown in figure 6.

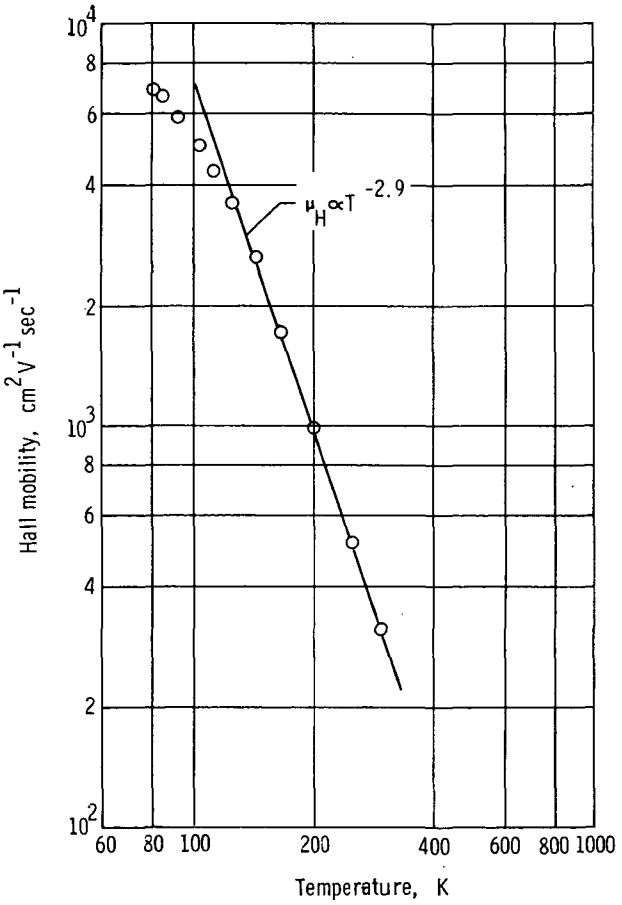

Figure 6.- Hall mobility as a function of temperature for beryllium-doped silicon.

The temperature dependence of the mobility indicates the dominant free-carrier scattering mechanism. If the scattering is primarily due to phonons, the mobility has a negative power dependency on the temperature; however, if ionized impurity scattering is dominant, the mobility will be a positive power function of the temperature (ref. 39). Here it is noted that the mobility is primarily controlled by phonon scattering down to temperatures around 80 K. When silicon is heavily compensated (on the order of 10^{16} cm^{-3}), the mobility is primarily controlled by phonon scattering down to temperatures of only 100 K or greater; therefore, the beryllium is typical of a p-type impurity with low or moderately low compensation levels.

Absorption studies in the infrared region of beryllium in silicon at low temperatures show that there are two series of sharp absorptions, located around 1450 cm^{-1} and 1080 cm^{-1} (labeled Set I and Set II, respectively) and a single broad absorption centered on 500 cm^{-1} (see fig. 7). The spacings between absorptions are typical of the spacings

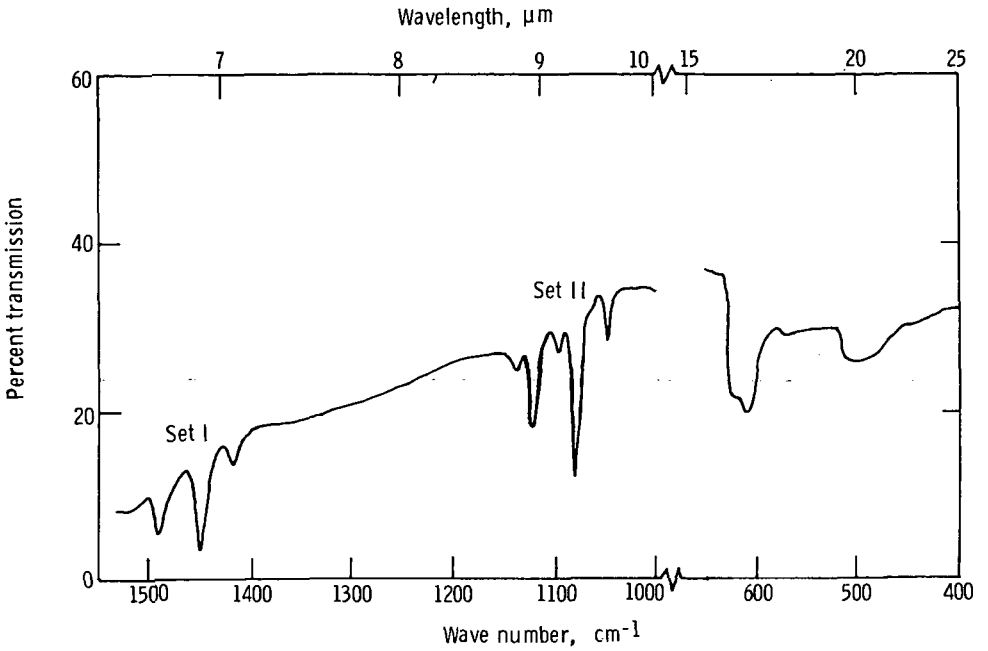

Figure 7.- Typical beryllium spectra showing Set I and Set II absorptions and the broad absorption band at 500 cm^{-1}.

observed for shallow acceptors in silicon as seen in table 2 and figure 2. If shallow-acceptor theory is applied, these two series correspond to ionization energies of 191 and 145 meV. This is in acceptable agreement with the value obtained from the Hall measurements.

As the temperature of the sample is raised, the Set I and Set II lines broaden quite rapidly as shown in figures 8(a) and 8(b). Resolution of the lines above 100 K was not

TABLE 2.- ENERGY LOCATION AND SPACINGS OF LINES IN TYPICAL BERYLLIUM AND BERYLLIUM-LITHIUM SPECTRA

Line	Boron	Indium	Beryllium		Beryllium-lithium	
			Set I (a)	Set II (a)	Set I (a)	Set II (a)
Energy location of location of lines, meV						
1	30.38	141.99	176.6	130.2	91.8	67.0
2	34.53	145.79	180.3	134.4	95.1	70.8
3	38.35	149.74		136.4	99.1	
4	39.64	150.80	185.6	139.7	100.4	76.1
	39.91	151.08				
5	41.52	152.8				
6	42.50	153.27				
7	42.79			141.9	103.0	
Energy spacings between lines, meV						
1 to 2	4.15	3.80	3.7	4.2	3.3	3.8
2 to 3	3.82	3.95		2.0	4.0	
2 to 4	5.11	5.01	5.3	5.3	5.3	5.3
4 to 7	3.15			2.2	2.6	

[a] Line designations are arbitrary.

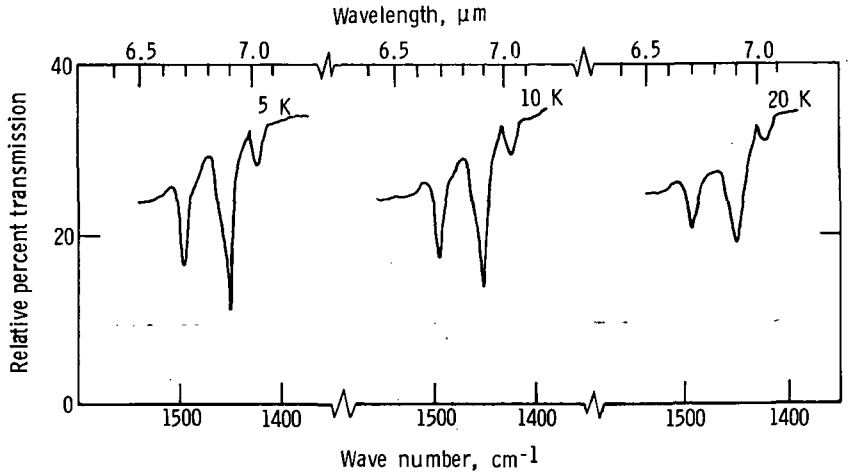

(a) Beryllium, Set I.

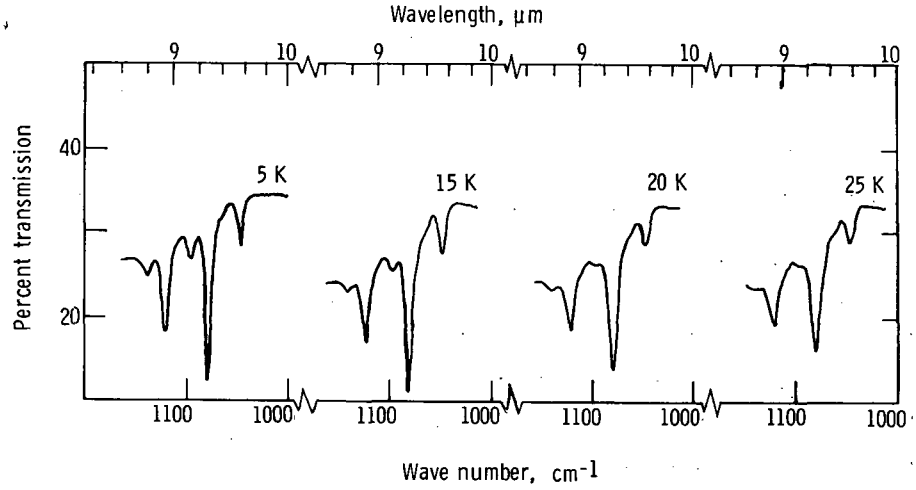

(b) Beryllium, Set II.

Figure 8.- Temperature dependence of absorptions.

possible. However, the broad line at 500 cm^{-1} does not seem to change very much with temperature, indicating that it is probably a localized impurity vibrational absorption associated with one of the beryllium centers (refs. 24 to 26).

As seen in table 2, the spacings of the major lines in the Set I and Set II absorptions are quite similar. The Set II series is always weaker than the Set I, never having an absorption coefficient greater than about one-half that of Set I. When a beryllium-doped sample is quenched from a temperature greater than about 600° C, the Set II series is drastically reduced or disappears while the Set I and 500 cm^{-1} lines increase slightly (fig. 9). When a sample is slowly cooled (on the order of 2 hr) from 600° C to room

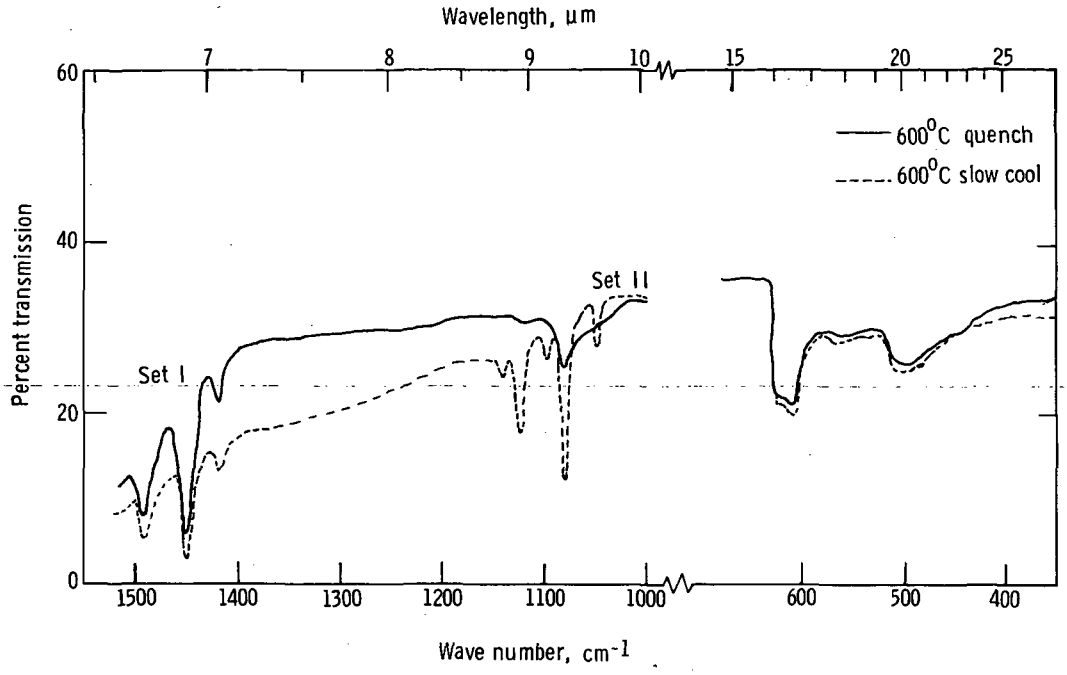

Figure 9.- Effects of quenching and annealing on beryllium, Set I and Set II.

temperature, the Set II series absorption is increased to its maximum value relative to Set I. Set I and the 500 cm^{-1} lines are slightly decreased in strength (fig. 9).

From these data it appears that the Set I and Set II series arise from two different configurations of the beryllium impurity atoms. Since the spacings between the lines are essentially the same and the ratio of the absorption coefficients can be changed, it is very unlikely that the Set II absorptions are the $p_{1/2}$ spectra as might be suspected at first. That is, transitions have previously been observed to states associated with the $p_{3/2}$ valence band and the $p_{1/2}$ valence band which are separated by about 44 meV ($\approx$355 cm^{-1}) (see fig. 1). However, it is unlikely that the spacings between lines would be so close or that the relative strengths of absorption would be affected by heat treatment.

It might be noted that beryllium is not unique in introducing more than one independent impurity level spectrum. Sulfur, when introduced into silicon, gives rise to four donor levels, at least two of which are unrelated (i.e., not the second level of a helium model), and whose relative absorptions are dependent on temperature histories (ref. 35).

Figure 9 indicates that the 500 cm^{-1} band is associated with the Set I impurity vibration as opposed to Set II since it generally tends to follow the behavior shown by Set I rather than Set II under quenching and annealing. When a beryllium-doped sample is isothermally annealed at temperatures greater than 1000° C, the Set I and 500 cm^{-1} absorptions decrease at about the same rate, so that after about 4 to 6 hr they both completely disappear due to out diffusion of the beryllium.

When beryllium is introduced into Czochralski-grown silicon (oxygen content typically 10^{18} cm^{-3}), the 9-μm absorption associated with interstitial oxygen completely disappears (fig. 10). The beryllium spectrum appears to be no different from that for the float-zone silicon (oxygen content less than 10^{16} cm^{-3}). Even after annealing for several hours to remove all the optically active beryllium, the 9-μm oxygen line is never fully recovered (i.e., the interstitial oxygen content in a position giving rise to the 9-μm line remains less than 0.1 its original value).

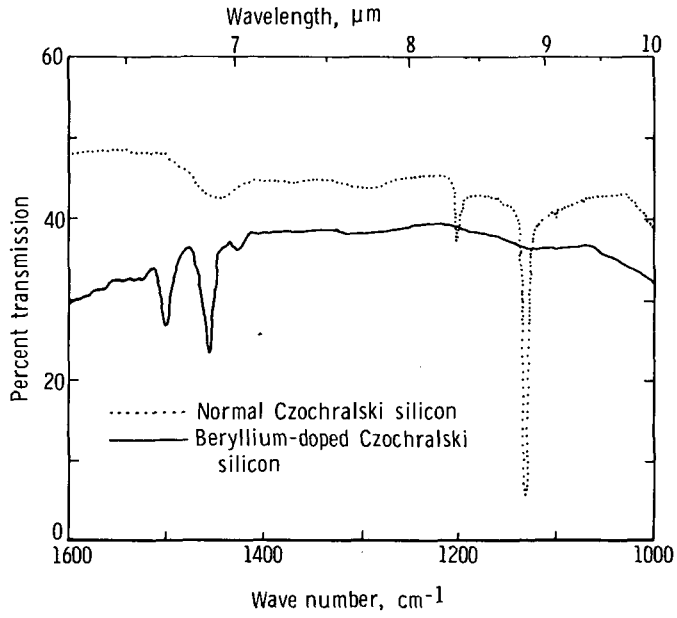

Figure 10.- Effect of beryllium on oxygen in Czochralski-grown silicon.

Beryllium-Lithium Complexes

When lithium is thermally diffused into silicon, it normally occupies an interstitial position and gives rise to a donor level. It is expected that lithium would compensate the beryllium impurities and allow study of the singly ionized beryllium states, expected if beryllium could be described by a helium model. After the lithium was introduced into beryllium-doped silicon, the samples were still p-type after diffusion for 1 hr at 600° C. Calculations from Hall data (fig. 11) indicated that the holes were bound in a level with an ionization energy E_A of about 108 meV. This may be compared with ionization energies which would be expected from compensation of the helium model, namely energies around 800 meV (≈6450 cm^{-1}). The mobility data shown in figure 12 exhibited very little of the ionized impurity scattering which would be expected for a highly compensated sample; in fact, the mobility in beryllium-lithium samples was essentially the same as for comparably doped beryllium samples.

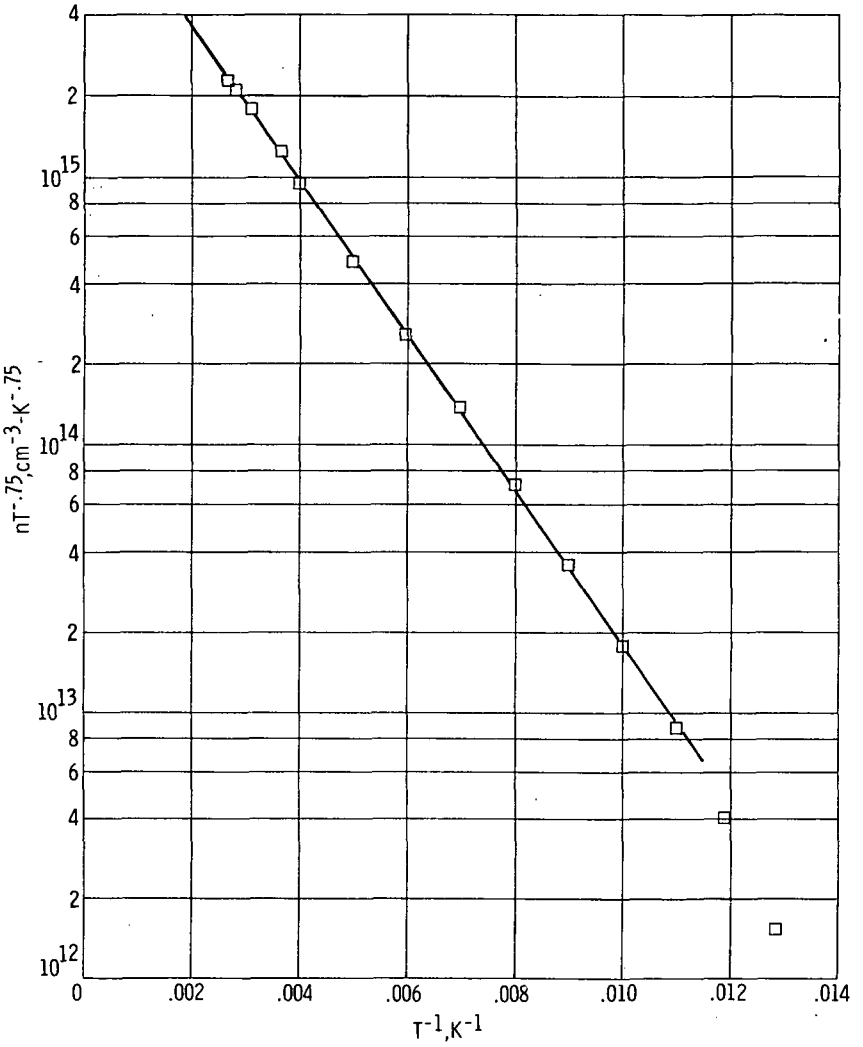

Figure 11.- Parameter containing carrier concentration and temperature as a function of temperature for a beryllium-lithium sample.

The suspicions that the introduction of lithium had caused something unusual were verified when the infrared spectrum of a beryllium-lithium-doped sample was observed. As shown in figure 13, two new series of acceptorlike absorptions were observed at ionization energies corresponding to 106 and 81 meV, respectively. The previously observed beryllium spectra were still there. In addition, the absorption around 500 cm^{-1} was asymmetric and had its minimum value at about 516 cm^{-1}.

The spacings between the lines of all four excited-state series are essentially the same (cf. table 2). After quenching a beryllium-lithium series from 600° C or greater, the intensities of the Set II lines are greatly reduced while the intensities of the beryllium-lithium series, Set I increase a little (see fig. 14). Similarly with a slow cool from 600° C, the beryllium-lithium absorptions, Set II are increased while the beryllium-lithium absorptions, Set I decrease very little.

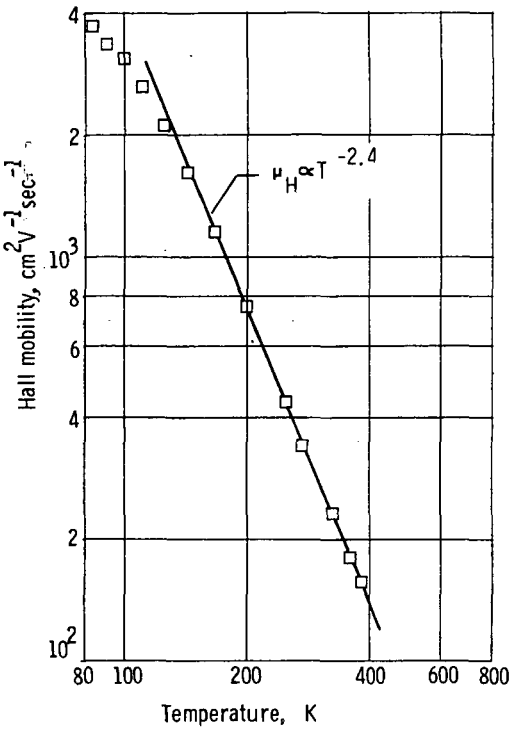

Figure 12.- Hall mobility as a function of temperature for a beryllium-lithium sample.

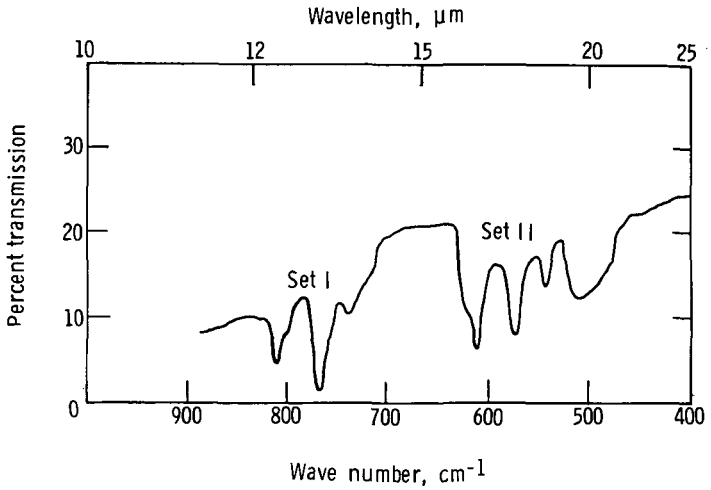

Figure 13.- Typical spectra showing beryllium-lithium absorptions, Set I and Set II.

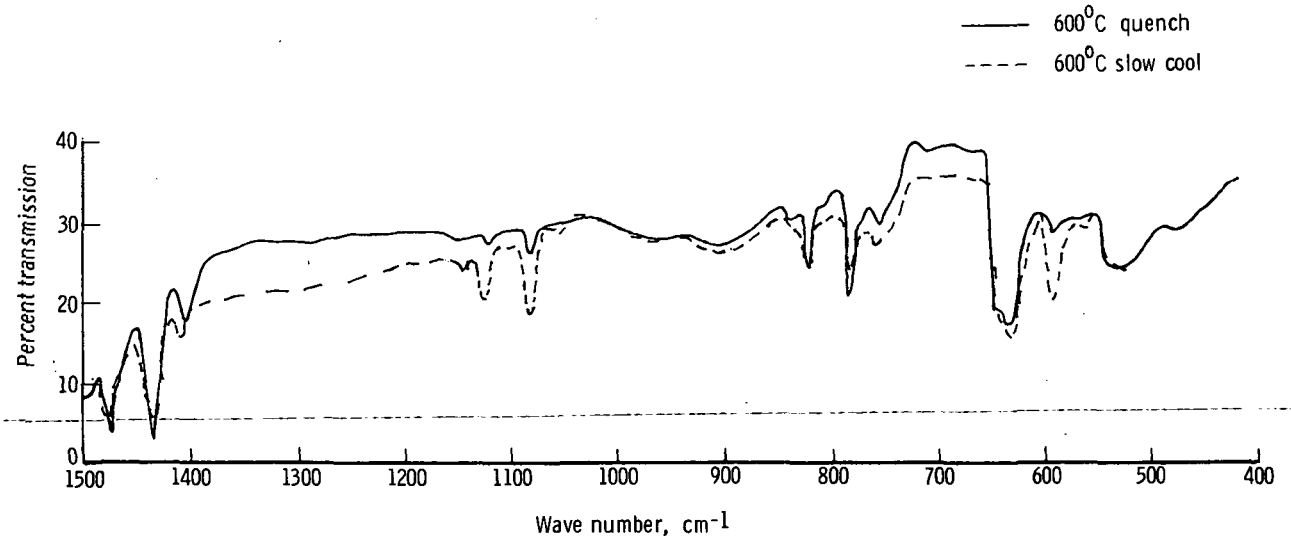

Figure 14.- Effects of quenching and annealing on beryllium-lithium absorptions, Set I and Set II.

As with the beryllium samples, the absorptions associated with beryllium-lithium broaden rapidly with increasing temperature and are unresolvable at temperatures greater than about 60 K to 70 K. However, as the sample temperature is increased, another series of lines appear which are displaced from the beryllium-lithium series, Set I by about 1.2 meV ($\approx$10 cm^{-1}) (see fig. 15).

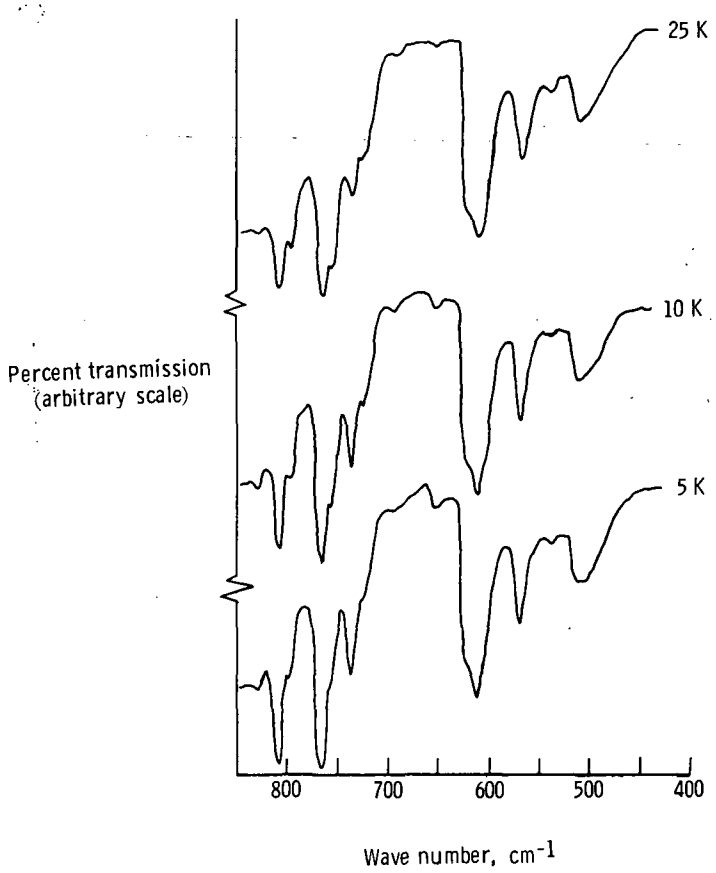

Figure 15.- Temperature dependence of beryllium-lithium absorptions, Set I and Set II.

The absorptions associated with beryllium-lithium, Set II do not seem to broaden as rapidly and do not show the second series. The appearance of the small absorptions in the beryllium-lithium, Set I is consistent with what would be expected if the fourfold degenerate ground state were split into two levels separated by 1.2 meV. As the temperature is raised, the upper level is populated by thermal excitation of the holes, and the transitions to the excited states can then be observed.

When lithium is introduced into a beryllium-doped Czochralski-silicon sample, the beryllium-lithium spectra are essentially the same as for the float-zone material. The spectra for a Czochralski sample are shown in figure 13. The beryllium-lithium, Set II lines are broad and lie in the vicinity of strong lattice absorptions which make accurate

determination of the spacings very difficult. It is felt that comparative spectra may be the best way to study accurately this series of absorptions.

PROPOSED MODELS

Beryllium

The very fast diffusion rate of beryllium in silicon indicates interstitial diffusion and leads one to expect beryllium to be an interstitial impurity. However, the addition of beryllium produces p-type silicon which indicates that the electrically active beryllium is in a substitutional position. Mass-spectroscopy data show that only about 10 percent of the beryllium contributes to the change in electrical and optical properties. It is believed that the other 90 percent of the beryllium is located in neutral sites, most likely close substitutional-interstitial beryllium pairs which would behave as neutral impurities. It appears that the beryllium diffuses interstitially but is trapped in the vacancies which are abundant at the doping temperature of 1300° C. When the beryllium is introduced into Czochralski-grown silicon, the interstitial beryllium interacts with the interstitial oxygen to form an interstitial beryllium-oxygen molecule. The bond energy of the beryllium-oxygen and the silicon-silicon bonds exceeds that of the silicon-oxygen-silicon bonds making the formation of the interstitial beryllium-oxygen energetically favorable.

Set I.- If a beryllium impurity atom were located on a substitutional lattice site, it would satisfy two of the covalent bonds with nearest neighbor silicon atoms. The remaining covalent bonds would capture electrons, but the entire center would remain neutral by binding two holes to the beryllium center on the lattice site which has a double negative charge (fig. 16). (Figures 16 to 21 are oversimplified for pedagogical reasons. In fact, the trapped electrons cannot be localized on any particular bond and the holes would be in orbit around the impurity center.) The holes would be several atomic diameters away and would be described in a simple way by effective-mass theory for a helium model. Therefore, when one of the holes is raised to an excited state, the spectra should look essentially like a Group III shallow acceptor. This is presumably what gives rise to the Set I absorptions. In the present context, the beryllium atom appears to be significantly smaller than the silicon atom. According to the theory of Morgan (ref. 15), this smaller atom will have a large local strain field associated with it which produces ground states much deeper than predicted by effective-mass theory.

When one of the holes is freed, leaving an ionized center, simple theory would predict that the second hole should be observable at an energy somewhere around four times that required to free the first hole. This type of behavior has been observed for the donors magnesium and sulfur in silicon and the acceptor zinc in germanium. In the case

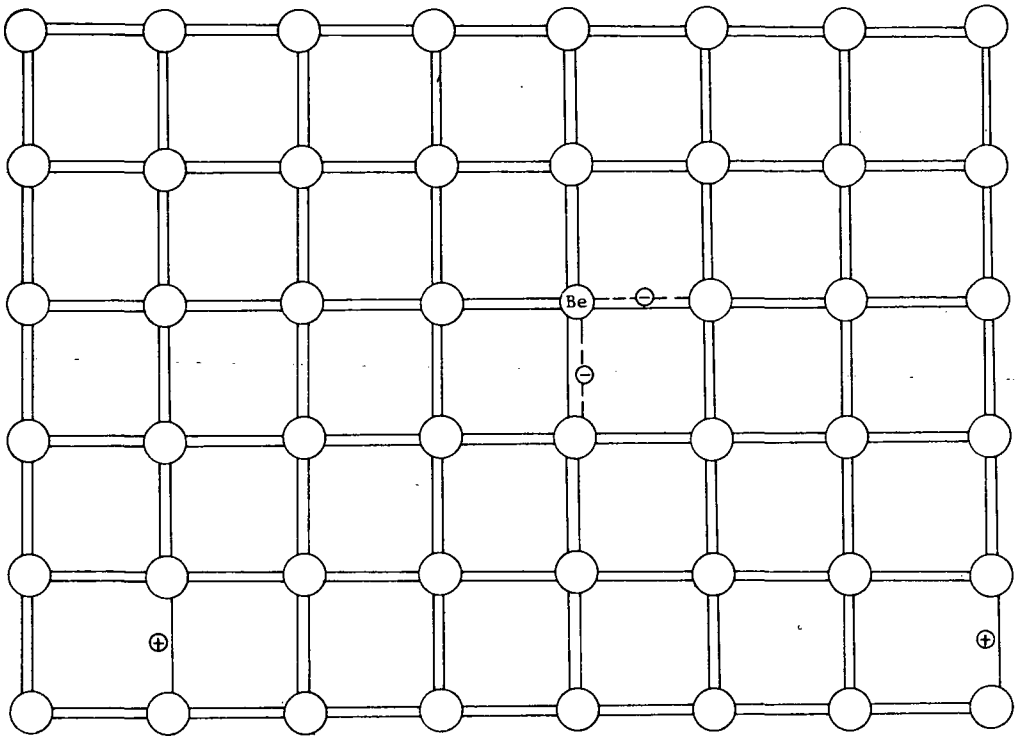

Figure 16.- Schematic model for neutral beryllium, Set I.

of beryllium, however, no such second level has been observed in this region. Several things could explain the absence of the second series of absorptions associated with the Set I lines.

One might start over by assuming that the beryllium is not in a substitutional site. This would require entirely new model concepts for the beryllium acceptor and would presumably complicate the model for the beryllium-lithium complex. On this basis, another explanation was sought. When the first hole is freed from the heliumlike model, the second hole will be attracted into a smaller orbit (see fig. 17). It is clearly possible that when the orbit becomes smaller, the assumption of a dielectric constant used in effective-mass theory becomes much weaker. The screening now seen by the hole could be much less than before, resulting in a much more tightly bound hole than predicted.

In addition, a lattice-symmetrical short-range potential (central-cell potential) would be much more effective for a hole located close to the impurity site. This potential would be used for calculating the ground-state energy for various impurities, and large values of the potential might possibly result in more tightly bound holes. In a theoretical paper, Ryabokon and Svidzinskii (ref. 14) state that for Group II impurities, ". . . the effective short-range potential turns out to be more effective in them and leads to quite large level shifts." Furthermore, they add that some of the deep impurity levels in silicon fall inside allowed energy bands. Thus, it seems possible for beryllium to be in a

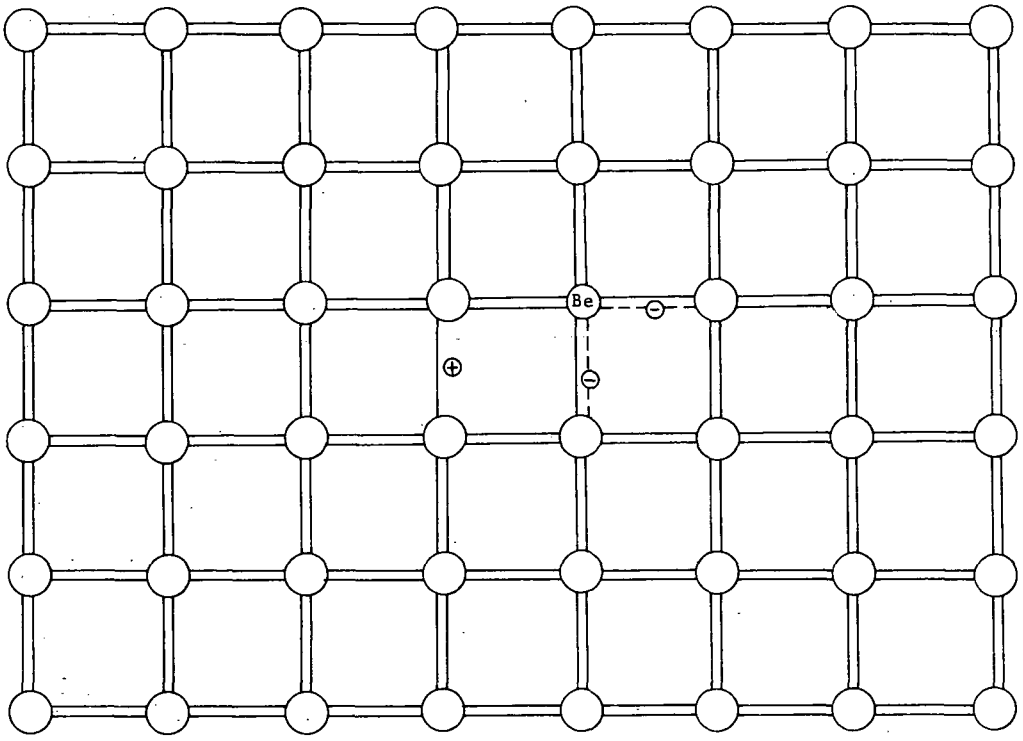

Figure 17.- Schematic model for singly ionized beryllium, Set I.

substitutional site, even though the second hole is not observed as predicted by the helium model.

Set II.- When a beryllium sample is quenched from high temperatures, the Set II absorptions are greatly reduced or disappear, and the Set I absorptions are enhanced. After a slow cool, the Set II absorptions are much stronger, and the Set I absorptions are slightly reduced. This seems to indicate that the Set II absorptions result from a more complex arrangement than Set I and that Set I absorptions are due to a component of impurities giving rise to Set II. It appears that the simplest model for the Set II absorptions is two beryllium atoms on nearest neighbor lattice sites. This configuration is somewhat similar to the divacancy bonding configurations, but less complex (see fig. 18). As the temperature of the sample is raised, the thermal energy of the lattice is such that the Set II sites are broken up into two Set I sites, that is, two substitutional beryllium sites. This results in a reduction of Set II absorptions after a quench. When the sample is slowly cooled, the beryllium atoms presumably tend to aggregate to relieve crystal stresses around the small beryllium impurity. Thus, more pairs are formed, and Set II absorptions are stronger after a slow cool. Again, the second hole associated with this model might not be observable in the infrared range (see fig. 19). These two models seem to be consistent with the optical and electrical data.

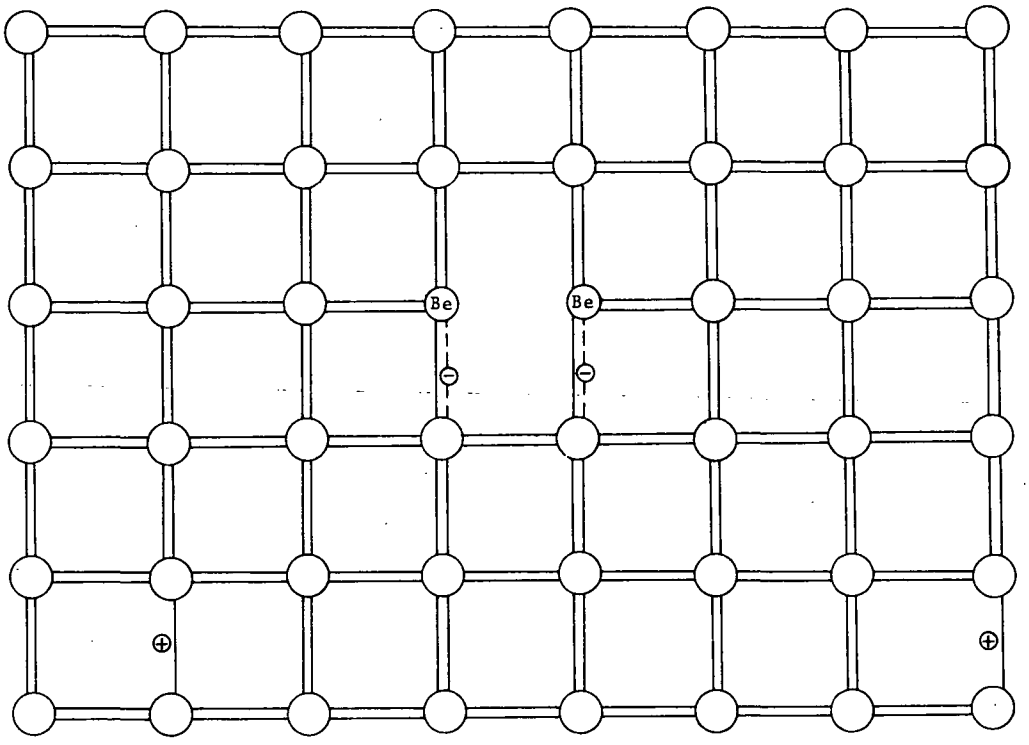

Figure 18.- Schematic model for neutral beryllium, Set II.

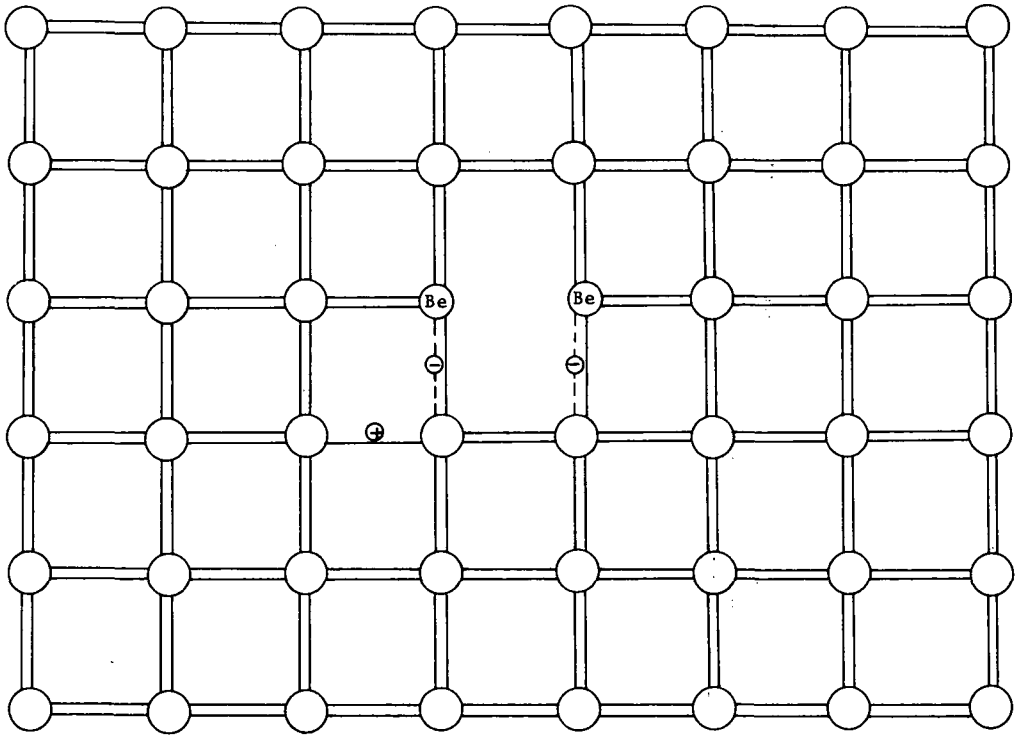

Figure 19.- Schematic model for singly ionized beryllium, Set II.

Set I.- When lithium is introduced into beryllium-doped silicon, an acceptor level with essentially the same spacings as the beryllium, Set I spectrum has been observed, but with the binding energy of the hole reduced by about 45 percent. It is believed that the lithium goes into one of the nearest neighbor interstitial tetrahedral sites (ref. 21) and its valence electron satisfies one of the unsatisfied covalent silicon bonds (fig. 20). The lithium in this position could reduce the local strain field, thus resulting in a lower ionization energy (ref. 15). While the short-range effects of the lithium are apparently large, the long-range effects should be quite small; therefore, the excited-state spectra should be essentially unaffected. Similarly, if the lithium is located in the immediate vicinity of the beryllium impurity, the ionic scattering from the complex center would be less than if the spacing between the two centers were large. That is, the beryllium-lithium center would be essentially a monovalent acceptor site.

As pointed out earlier, there is an apparent splitting of the ground state for the loosely bound hole in beryllium-lithium samples. If the lithium is in the immediate vicinity of the beryllium, the interaction between the beryllium and lithium ions would most likely be directed along a bond or <111> axis. In effect, this would be equivalent to a uniaxial stress applied in the <111> direction. As reported in reference 8, a <111> stress

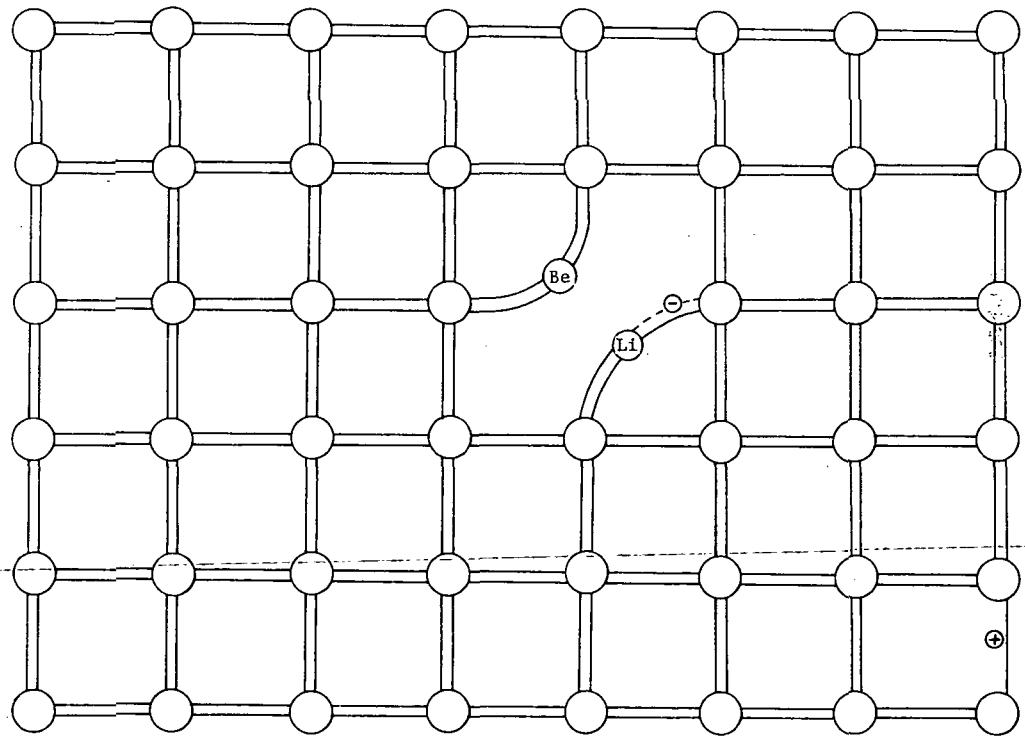

Figure 20.- Schematic model for neutral beryllium-lithium complex, Set I.

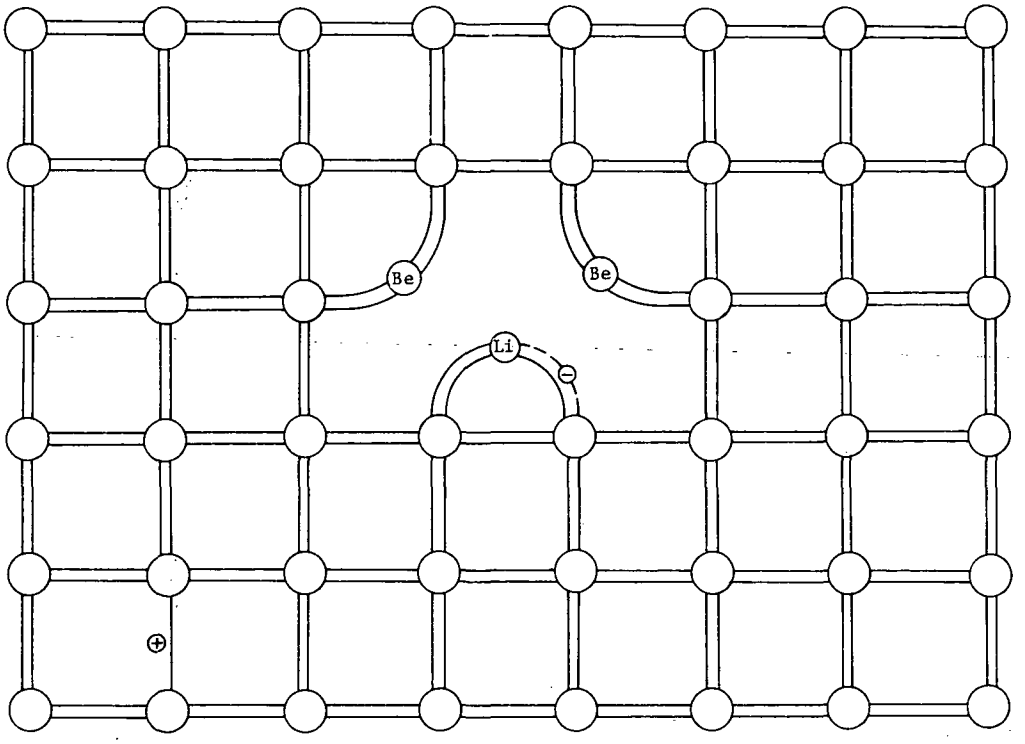

Figure 21.- Schematic model for neutral beryllium-lithium complex, Set II.

causes the ground state to split into two levels. Since these stresses are local, the excited states would not be split. This is in agreement with what is observed.

Set II.- When lithium comes into the vicinity of the beryllium, Set II, its valence electron again goes into one of the unsatisfied silicon convalent bonds, removing what would correspond to the deep hole (see fig. 21). The result, as before, would be to reduce the binding energy of the remaining hole. The mobility would not be affected by this configuration because no new ionic scattering centers have been introduced.

If this model is accurate, the complex would probably not have a <111> symmetry when the lithium is introduced; but the model for the beryllium complex, Set II would have a <111> axis of symmetry. However, the ground state for a heliumlike model would not have the same degeneracy as the Group III acceptors; and in fact, it is likely that both the beryllium, Set I and Set II will have only twofold degenerate ground states. The lithium should reduce even further the symmetry of the beryllium, Set II center, but the ground state would probably remain twofold degenerate (ref. 8).

CONCLUDING REMARKS

Beryllium as an impurity in silicon gives rise to two acceptor levels and associated excited-state levels referred to as Set I and Set II. The ratio of the absorption coeffi-

cients between Set I and Set II can be changed by quenching or annealing. Analysis of these studies indicates that the Set II absorptions are due to an impurity complex and that the Set I absorptions are due to a component of the Set II complex.

When lithium is introduced into the beryllium-silicon system, it gives rise to two new acceptor levels. These levels behave under quenching and annealing just like the beryllium, Set I and Set II levels. The beryllium-lithium, Set I ground state is split into two levels.

The following models, which seem to be the simplest impurity configurations that agree qualitatively with all the observations, are proposed to explain these four defects:

1. For beryllium, Set I, this defect is a single substitutional beryllium impurity. The second hole of a heliumlike model is so tightly bound that it cannot be found in the region predicted by shallow-acceptor theory.

2. For beryllium, Set II, this defect is made up of two beryllium atoms on nearest neighbor substitutional sites. Again, a deep hole may be associated with the level; but the hole could be so tightly bound that it falls inside the allowed energy bands.

3. For beryllium-lithium, Set I, the lithium ion is trapped in the immediate vicinity of the beryllium, Set I and removes the deep hole. The symmetry of the impurity site is reduced, resulting in the reduction of the degeneracy of the ground state and the splitting of this level.

4. For beryllium-lithium, Set II, the lithium removes the deep hole as in Set I; but the ground-state degeneracy is not reduced because of the different symmetries associated with the beryllium, Set I and Set II sites.

Langley Research Center,
National Aeronautics and Space Administration,
Hampton, Va., November 20, 1972.

REFERENCES

1. Pearson, G. L.; and Bardeen, J.: Electrical Properties of Pure Silicon and Silicon Alloys Containing Boron and Phosphorus. Phys. Rev., vol. 75, no. 5, Mar. 1, 1949, pp. 865-883.

2. Morin, F. J.; and Maita, J. P.: Electrical Properties of Silicon Containing Arsenic and Boron. Phys. Rev., vol. 96, no. 1, Oct. 1, 1954, pp. 28-35.

3. Morin, F. J.; Maita, J. P.; Shulman, R. G.; and Hannay, N. B.: Impurity Levels in Silicon. Phys. Rev., Second ser., vol. 96, no. 3, Nov. 1, 1954, p. 833.

4. Long, Donald; and Myers, John: Hall Effect and Impurity Levels in Phosphorus-Doped Silicon. Phys. Rev., vol. 115, no. 5, Sept. 1, 1959, pp. 1119-1121.

5. Hrostowski, H. J.; and Kaiser, R. H.: Infrared Spectra of Group III Acceptors in Silicon. J. Phys. & Chem. Solids, vol. 4, 1958, pp. 148-153.

6. Picus, G.; Burstein, E.; and Henvis, B.: Absorption Spectra of Impurities in Silicon – II. Group-V Donors. J. Phys. & Chem. Solids, vol. 1, 1956, pp. 75-81.

7. Aggarwal, R. L.; and Ramdas, A. K.: Effect of Uniaxial Stress on the Excitation Spectra of Donors in Silicon. Phys. Rev., Second ser., vol. 137, no. 2A, Jan. 18, 1965, pp. A602-A612.

8. Onton, A.; Fisher, P.; and Ramdas, A. K.: Spectroscopic Investigation of Group-III Acceptor States in Silicon. Phys. Rev., vol. 163, no. 3, Nov. 15, 1967, pp. 686-703.

9. Kohn, W.; and Luttinger, J. M.: Theory of Donor States in Silicon. Phys. Rev., vol. 98, no. 4, May 15, 1955, pp. 915-922.

10. Kleiner, Walter H.: Excited Donor Levels in Silicon. Phys. Rev., vol. 97, no. 6, Mar. 15, 1955, pp. 1722-1723.

11. Schechter, D.: Theory of Shallow Acceptor States in Si and Ge. J. Phys. & Chem. Solids, vol. 23, 1962, pp. 237-247.

12. Kohn, W.: Shallow Impurity States in Silicon and Germanium. Solid State Physics, Vol. 5, Frederick Seitz and David Turnbull, eds., Academic Press, Inc., 1957, pp. 257-320.

13. Narita, Koziro; and Shimizu, Tatsuo: Ground State Energies of Donors in Ge and Si. J. Phys. Soc. Jap., vol. 16, 1961, p. 2588.

14. Ryabokon', V. N.; and Svidzinskii, K. K.: Theory of Deep Acceptor Levels in Semiconductors. Sov. Phys. – Solid State, vol. 11, no. 3, Sept. 1969, pp. 473-478.

15. Morgan, T. N.: Shallow Acceptor States in Semiconductors – The Local Strain Field. Proceedings of the Tenth International Conference on the Physics of Semiconductors, Seymour P. Keller, John C. Hensel, and Frank Stern, eds., CONF-700801, U.S. At. Energy Comm., Oct. 1970, pp. 266-271.

16. Kaiser, W.; and Keck, P. H.: Oxygen Content of Silicon Single Crystals. J. Appl. Phys., vol. 28, no. 8, Aug. 1957, pp. 882-887.

17. Hrostowski, H. J.; and Kaiser, R. H.: Infrared Absorption of Oxygen in Silicon. Phys. Rev., vol. 107, no. 4, Aug. 15, 1957, pp. 966-972.

18. Hrostowski, H. J.; and Alder, B. J.: Evidence for Internal Rotation in the Fine Structure of the Infrared Absorption of Oxygen in Silicon. J. Chem. Phys., vol. 33, no. 4, Oct. 1960, pp. 980-990.

19. Crouch, Roger Keith; and Gilmer, T. E., Jr.: Thermal Ionization Energy of Lithium and Lithium-Oxygen Complexes in Single-Crystal Silicon. J. Phys. & Chem. Solids, vol. 30, 1969, pp. 2037-2043.

20. Gilmer, T. E., Jr.; Franks, R. K.; and Bell, R. J.: An Optical Study of Lithium and Lithium-Oxygen Complexes as Donor Impurities in Silicon. J. Phys. & Chem. Solids, vol. 26, 1965, pp. 1195-1204.

21. Aggarwal, R. L.; Fisher, P.; Mourzine, V.; and Ramdas, A. K.: Excitation Spectra of Lithium Donors in Silicon and Germanium. Phys. Rev., vol. 138, no. 3A, May 3, 1965, pp. A882-893.

22. Pell, E. M.: Interactions Between Li and O in Si. Solid State Physics in Electronics and Telecommunications, Vol. 1 – Semiconductors, Pt. 1, M. Desirant and J. L. Michiels, eds., Academic Press, Inc., 1960, pp. 261-276.

23. Chrenko, R. M.; McDonald, R. S.; and Pell, E. M.: Vibrational Spectra of Lithium-Oxygen and Lithium-Boron Complexes in Silicon. Phys. Rev., vol. 138, no. 6A, June 14, 1965, pp. A1775-1784.

24. Balkanski, M.; and Nazarewicz, W.: Localized Vibration Due to Boron and Lithium in the Silicon Lattice. J. Phys. & Chem. Solids, vol. 25, 1964, pp. 437-441.

25. Waldner, M.; Hiller, M. A.; and Spitzer, W. G.: Infrared Combination Mode Absorption in Lithium-Boron-Doped Silicon. Phys. Rev., vol. 140, no. 1A, Oct. 4, 1965, pp. A172-176.

26. Newman, R. C.; and Smith, R. S.: Vibrational Absorption of Carbon and Carbon-Oxygen Complexes in Silicon. J. Phys. & Chem. Solids, vol. 30, 1969, pp. 1493-1505.

27. Tyapkina, N. D.; Krivopolenova, M. M.; and Vavilov, V. S.: Electrical Properties of p-Type Germanium Containing Beryllium. Sov. Phys. – Solid State, vol. 6, no. 7, Jan. 1965, pp. 1732-1733.

28. Sidorov, V. I.; Sushko, T. E.; and Shul'man, A. Ya.: Investigation of Optical Absorption in Germanium Doped With Zinc and Compensated With Antimony. Sov. Phys. – Solid State, vol. 8, no. 7, Jan. 1967, pp. 1608-1610.

29. Fisher, P.; and Fan, H. Y.: Absorption Spectra and Zeeman Effect of Copper and Zinc Impurities in Germanium. Phys. Rev. Lett., vol. 5, no. 5, Sept. 1, 1960, pp. 195-197.

30. Robertson, J. B.; and Franks, R. K.: Beryllium as an Acceptor in Silicon. Solid State Commun., vol. 6, 1968, pp. 825-826.

31. Robertson, James B.: The Effect of Beryllium on Oxygen in Silicon. Bull. Amer. Phys. Soc., ser. II, vol. 13, no. 11, Nov. 1, 1968, p. 1475.

32. Franks, R. K.; and Robertson, J. B.: Magnesium as a Donor Impurity in Silicon. Solid State Commun., vol. 5, 1967, pp. 479-481.

33. Ho, L. T.; and Ramdas, A. K.: Excitation Spectra and Piezospectroscopic Effects of Magnesium Donors in Silicon. Phys. Rev. B, vol. 5, no. 2, Jan. 15, 1972, pp. 462-474.

34. Taft, E. A.; and Carlson, R. O.: Beryllium as an Acceptor in Silicon. J. Electrochem. Soc.: Solid State Sci., vol. 117, no. 5, May 1970, pp. 711-713.

35. Krag, W. E.; Kleiner, W. H.; Zeiger, H. J.; and Fischler, S.: Sulfur Donors in Silicon: Infrared Transitions and Effects of Calibrated Uniaxial Stress. J. Phys. Soc. Jap., vol. 21, suppl. 1966, pp. 230-233.

36. Schultz, M. L.: Silicon: Semiconductor Properties. Infrared Phys., vol. 4, 1964, pp. 93-112.

37. Bauman, Robert P.: Absorption Spectroscopy. John Wiley & Sons, Inc., c.1962.

38. Valdes, L. B.: Resistivity Measurements on Germanium for Transistors. Proc. IRE, vol. 42, no. 2, Feb. 1954, pp. 420-427.

39. McKelvey, John P.: Solid State and Semiconductor Physics. Harper & Row, Publ., c.1966, pp. 308-319.

NATIONAL AERONAUTICS AND SPACE ADMISTRATION
WASHINGTON, D.C. 20546

OFFICIAL BUSINESS
PENALTY FOR PRIVATE USE $300

FIRST CLASS MAIL

POSTAGE AND FEES PAID
NATIONAL AERONAUTICS AND
SPACE ADMINISTRATION

U.S.MAIL

NASA 451

POSTMASTER: If Undeliverable (Section 158 Postal Manual) Do Not Return

"The aeronautical and space activities of the United States shall be conducted so as to contribute . . . to the expansion of human knowledge of phenomena in the atmosphere and space. The Administration shall provide for the widest practicable and appropriate dissemination of information concerning its activities and the results thereof."

—NATIONAL AERONAUTICS AND SPACE ACT OF 1958

NASA SCIENTIFIC AND TECHNICAL PUBLICATIONS

TECHNICAL REPORTS: Scientific and technical information considered important, complete, and a lasting contribution to existing knowledge.

TECHNICAL NOTES: Information less broad in scope but nevertheless of importance as a contribution to existing knowledge.

TECHNICAL MEMORANDUMS: Information receiving limited distribution because of preliminary data, security classification, or other reasons.

CONTRACTOR REPORTS: Scientific and technical information generated under a NASA contract or grant and considered an important contribution to existing knowledge.

TECHNICAL TRANSLATIONS: Information published in a foreign language considered to merit NASA distribution in English.

SPECIAL PUBLICATIONS: Information derived from or of value to NASA activities. Publications include conference proceedings, monographs, data compilations, handbooks, sourcebooks, and special bibliographies.

TECHNOLOGY UTILIZATION PUBLICATIONS: Information on technology used by NASA that may be of particular interest in commercial and other non-aerospace applications. Publications include Tech Briefs, Technology Utilization Reports and Technology Surveys.

Details on the availability of these publications may be obtained from:

SCIENTIFIC AND TECHNICAL INFORMATION OFFICE

NATIONAL AERONAUTICS AND SPACE ADMINISTRATION

Washington, D.C. 20546